CHAPTER 4

NEURAL NETWORK CONTROLLER FOR THE DRIVETRAIN SYSTEM

4.1 Introduction

A CVT will enable the engine to run at its fuel-efficient operating point for any vehicle load, due to its wide range of transmission ratio coverage. Most current metal pushing V-belt CVT are hydraulically actuated. Unfortunately, this type of CVT needs continuous force to keep the CVT pulleys clamping the metal belt and prevent belt slip. This continuous energy consumption becomes the major loss in hydraulic CVT system that could reduce CVT efficiency (Akerhurst *et al.,*1999). To overcome this energy loss, an electromechanical actuated CVT system could be a viable solution, since this system only operates during transmission ratio change. The electromechanical actuated CVT with a single acting pulley system has been shown to cause belt misalignment (Tawi, 1997; Meerakker *et al*., 2004). Slightly different than Meerakker, this research introduces a new electromechanical CVT with dual acting pulley system, utilizing two DC motors as actuators. This system adopts two movable pulley sheaves in both primary and secondary shafts to keep the belt position aligned at the centre of the shafts, even during transmission ratio change, hence eliminating belt misalignment effects. The electromechanical system is used, because this system has a viable solution for reducing power consumption compared with the hydraulic system (Meerakker *et al.*, 2004).

EMDAP-CVT enables a wide range of speed ratio change and it can adjust the ratio continuously and automatically according to the running condition and maintain the engine to work in economy mode or power mode at all time. The difficulty of EMDAP-CVT control system is to implement an optimal match between

engine and transmission system. The current technology of CVT is still maturing in theory, as well as in practice (Lin and Ren, 2001; Meilan *et al*., 2006).

The aim of this chapter is to propose and develop an EMDAP-CVT control strategy so that the engine speed can be maintained constant at it's desired speed by adjusting EMDAP-CVT ratio. Selecting the desired EMDAP-CVT ratio is done by an adaptive artificial neural network (ANN) controller for the outer loop control. PID controller is used as the inner loop controller to control the DC motor position.

4.2 The Proposed Drivetrain Controller

The development of drivetrain model has been discussed in Chapter 3, where the vehicle speed is controlled by the throttle opening, $\theta_{throttle}$, and the desired gear ratio, υ. Any external disturbance either comes from road profile or headwind will effect the vehicle speed as well as engine speed. Figure 4.1 shows a typical transmission ratio performance for maximum engine power when the throttle is fully opened (WOT) based on Daihatsu Mira 660 cc engine.

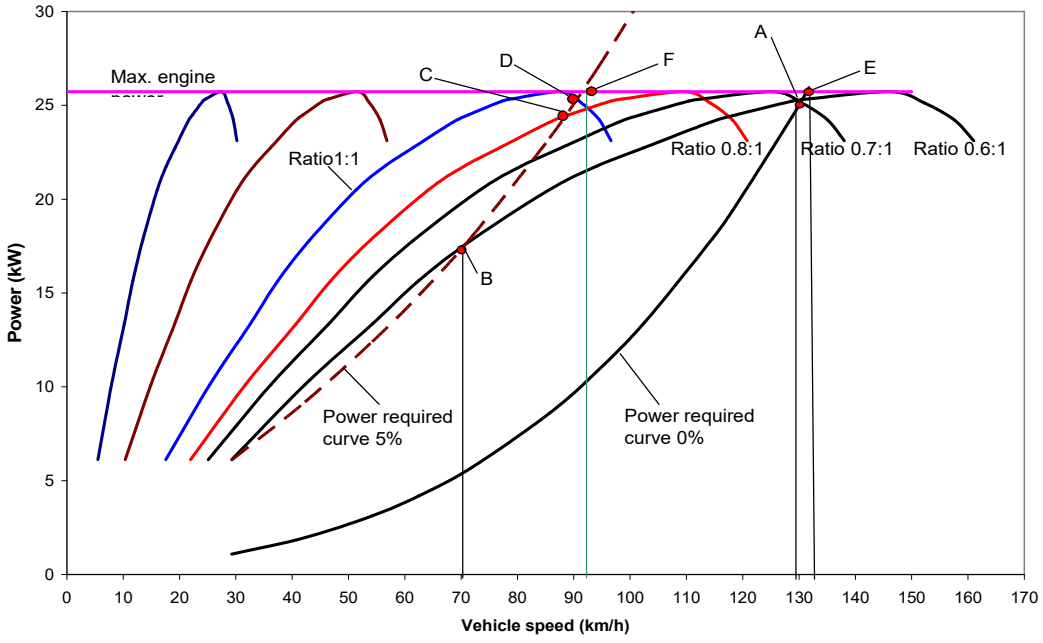

Figure 4.1 Calculated of typical transmission ratio performance for maximum engine power based on Daihatsu Mira 660 cc engine.

When a vehicle is moving on a flat road, the maximum speed achieved for a gear ratio of 0.6:1 is 130 km/h as shown by point A, which is the intersection between power required at 0% road gradient and gear ratio 0.6:1 curve. However, at point A the engine power is not at the maximum engine power. The control strategy is to ensure the engine speed operates at its maximum engine power. For maximum engine power requirement, the required gear ratio is given by point E, which is in-between 0.7:1 and 0.6:1 of the discrete gears. For discrete gear system, the transmissions with either settle to gear ratio of 0.7:1 or 0.6:1 which will result with the engine speed not operates at the maximum engine power. Similarly, if the road slope is 5%, the power required to overcome the load is shown by power required curve 5%. For a constant gear ratio of 0.6:1 the vehicle speed will be 70 km/h as given by point B. Using the same control strategy, the required gear ratio is given by the point of intersection between the power required line and the maximum power line at point F. For discrete gear ratio transmission this cannot be achieved since the gear ratio of 1:1 is given by point D and 0.8 is given by point C, which do not meet the maximum engine power requirement. Therefore, the control strategy that ensures the engine speed is at the maximum engine power can only be achieved using CVT, where the power line saturates at the maximum engine power once the low gear reach the maximum power. The intelligent controller designed and developed in this study is to implement this strategy.

With this control rule, two controller algorithms are proposed as an outer loop controller namely PID controller and a neural network controller. The classical PID controller is used as a benchmark to study the performance of the proposed outer loop controller. Figure 4.2 shows the control scheme of PID classical control as the outer loop controller. The alternative controller proposed is the adaptive neural network controller as shown in Figure 4.3.

The control scheme consists of an inner loop and an outer loop sub-systems. The inner loop control system is used to rotate the two DC motors independently and accordingly to obtain the desired ratio. The inner loop controller is the same for both control schemes. The outer loop control system evaluates the interaction between the engine, EMDAP-CVT and load dynamics as well as the driver's demand and road

condition and produces the desired ratio used by the inner loop control system as its input.

In the inner loop, although the clamping force required by the pair of pulley sheaves to hold the metal belt without slip is almost 20 kN, with the used of the gear reduction and power screw mechanism, classical control such as PD controller is sufficient to control the two DC motors with output torque of 1 Nm.

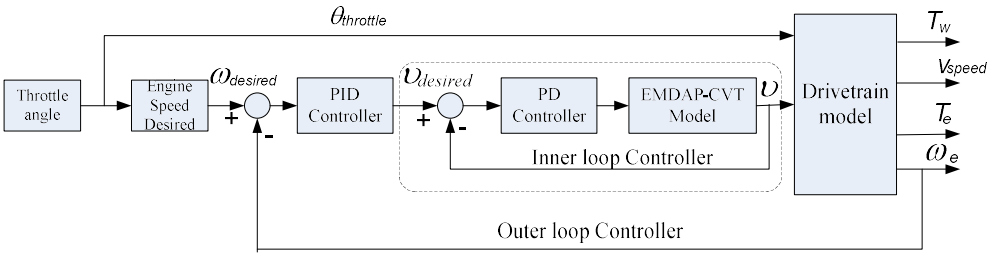

Figure 4.2 PID controller used for outer loop drivetrain control

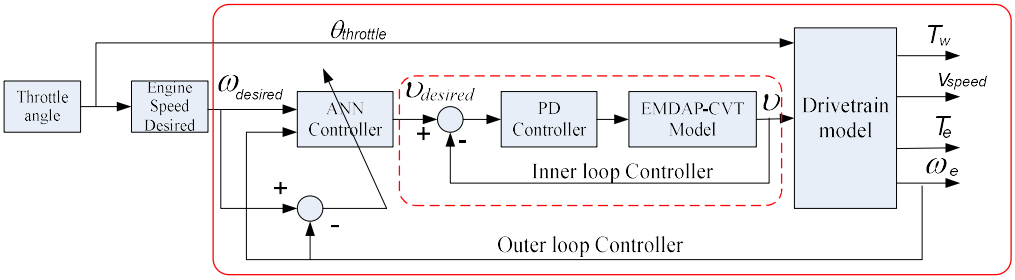

Figure 4.3 Adaptive ANN controller used for outer loop drivetrain control

4.3 Inner Loop Control System

The electromechanical dual acting pulley CVT (EMDAP CVT) system utilizes two DC motors as actuators. These two DC motors have to be control independently and accordingly to produce the desired ratio. The input shaft with input pulley sheaves is designed in such a way that the displacement of the moveable power screws is the same as the pulley sheave. The rotation of the primary DC motor can directly measure the displacement of the primary pulley sheave; hence the

measure of the radius of the belt at the primary pulley will determine the EMDAP-CVT ratio.

4.3.1 Strategising the Rotation DC Motors

The length of the metal pushing V-belt is always constant, but the relationship between input pulley radius and output pulley radius is non linear (see Appendix C), hence a more advance control strategy for the DC motor is needed. The output shaft with secondary pulley sheaves has been designed to reduce slip due to transient force during ratio change. A spring disc is inserted at the back of each secondary pulley sheave to provide a continuous clamping force.

Belt analysis is described in Appendix C. The belt radius at the primary pulley is not equal to the radius at the secondary pulley, and hence the rotation of DC motor for the primary pulley should not be equal to the secondary pulley as shown in Figure 4.4. Strategising the rotation of the two DC motors is handled by the inner loop controller using PD type controller.

Figure 4.4 shows that the rotation of the primary DC motor is not equal to the rotation of the secondary DC motor. When the EMDAP-CVT ratio is in underdrive position, the secondary DC motor encoder must be 788.29 and the primary DC motor encoder must be in the zero position. Conversely if the EMDAP-CVT ratio is at maximum overdrive, the primary DC motor encoder has the value of 900 and secondary DC motor encoder must be in zero position. The curves shown in Figure 4.4 are used as the reference for the two DC motors to rotate in order to obtain the desired EMDAP-CVT ratio. Because the transient force has been overcome by the disc spring, the rotation of both DC motors can either be rotated simultaneously or with delay.

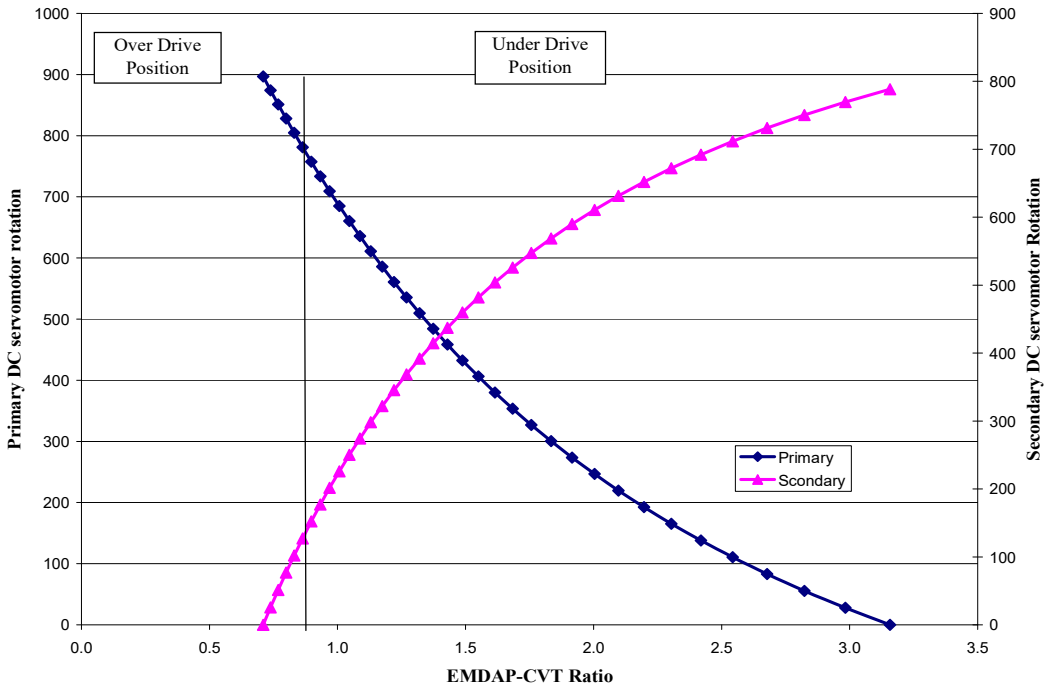

Figure 4.4 EMDAP-CVT ratio based on the DC motor rotation.

4.3.2 PID Controller

PID (Proportional, Intergral and Derivative) controller has been widely used in simple linear control systems. A basic PID controller is shown in Figure 4.5. The PID controller is a well known and well–established technique applied in various industrial control applications. This is mainly due to its simple design, straightforward parameters tuning, and robust performance. As actuators, DC motors are extensively used in many automatic control systems, including drive for robotic manipulators, machine tools, rolling machines, photocopy machines etc. PID controllers are usually used to control these motors. Position controls utilizing PID can be found in Jingzhuo *et al.,* (2000), Habib and Maki (2001), Yang *et al.,* (2002), and Yusuf *et al.,* (2003). To design an effective PID controller, three gain parameters, namely, proportional, integral and derivative gains need to be specified properly. The conventional approach to determine the PID parameters is to study the mathematical model of the process and try to use a simple tuning parameters that provides a fixed set of gain parameters. One famous example of such approach is the Ziegler-Nichols method (Hyung-Soo *et al.*, 1999).

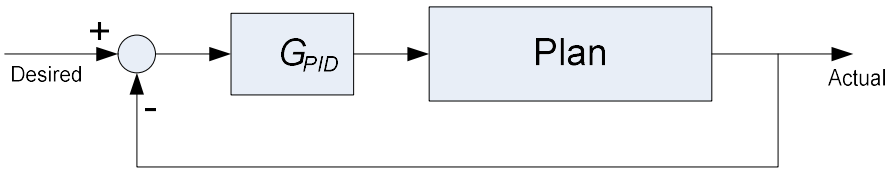

Figure 4.5 A general PID control scheme

The ideal continuous transfer function of a PID (G_{PID}) controller is given by

$$G_{PID} = K_p\left(e + \frac{1}{T_i}\int_0^t e\,dt + T_d\frac{de}{dt}\right) \tag{4.1}$$

where,

$T_i = K_p/K_i$

$T_d = K_d/K_p$

e : the error between the reference and the output signal system

T_i : the integral time

T_d : the derivative time

K_p : proportional gain

K_i : integral gain

K_d : derivative gain

In digital control and for small time sampling (T_s), the equation can be approximated by

$$G_{PID_n} = K_p\left(e_n + \frac{T_s}{T_i}\sum_{j=1}^{n} e_j + T_d\frac{e_n - e_{n-1}}{T_s}\right) \tag{4.2}$$

where, index n refers to the time instant. In order to get the suitable values of K_p, K_i, and K_d parameters, Ziegler-Nichols method can be used.

4.3.3 Simulink Block Diagram of EMDAP-CVT

Figure 4.6 shows the complete Simulink diagram of EMDAP-CVT with PD controller to control the position of the DC motor. This block diagram is built based on rotation of the two DC motors independently and accordingly. Each of the DC motor rotates to achieve its position by tracking the curve as shown in Figure 4.4. Two functions; (GRset to Rp_set) and (Rp_set to Xp_set); are used to determine the pulley sheave position. The position of secondary DC motor is determined using function (Xp_act to Xs_set) based on the secondary pulley curve shown in Figure 4.4.

By controlling the two DC motor positions the ratio change of EMDAP-CVT can be controlled according to the desired ratio to keep the engine speed constant although in the presence of vehicle load.

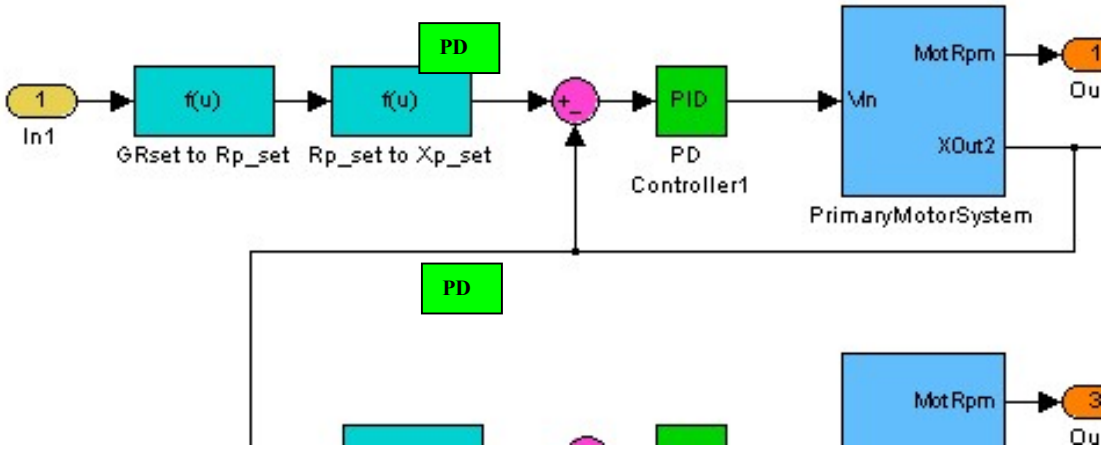

Figure 4.6 Simulink block diagram of EMDAP-CVT with PD

4.3.4 Performance of Inner Loop Controller

Figure 4.7 shows the simulation results of the performance of PD controller for the EMDAP-CVT ratio change from a low gear to a high gear. The PD gains were obtained using Ziegler-Nichols method with the value of 120 and 20 respectively. The time required to reach high gear from low gear is almost 10 seconds and vice versa. With this response of almost 10 second, the PD controller is

quite sufficient to be used as the inner loop controller. Because for the vehicle acceleration performance where the car with manual transmission reaches the speed of 100 km/h within 10 second, it can be reached by using transmission ratio up to 3rd gear ratio instead of 5th gear ratio. Due to the dynamic behaviour of the system it is almost impossible to follow the trajectory of a pulse generator exactly. In real implementation, the EMDAP-CVT ratio change is gradual as shown in Figure 4.8 in the form of triangle.

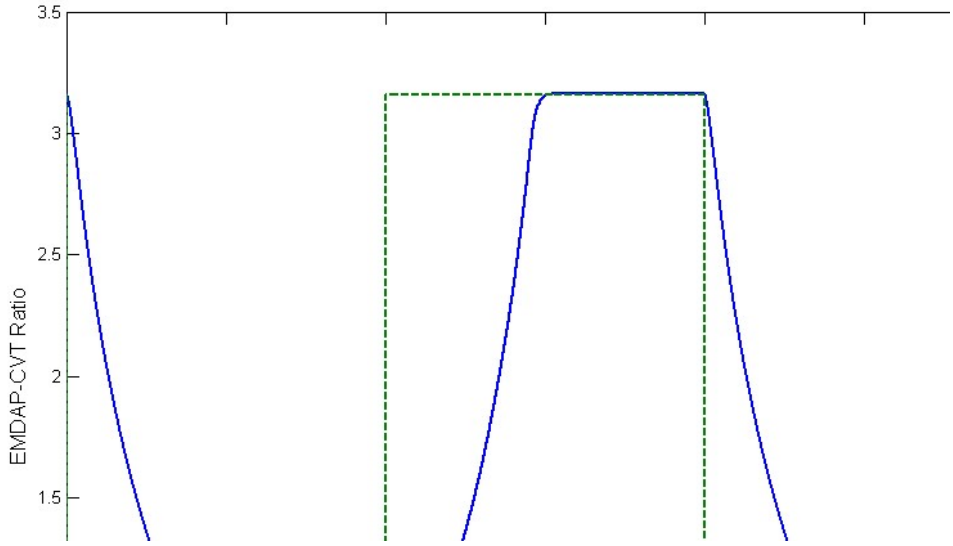

Figure 4.7 The response of PD controller with pulse generator input

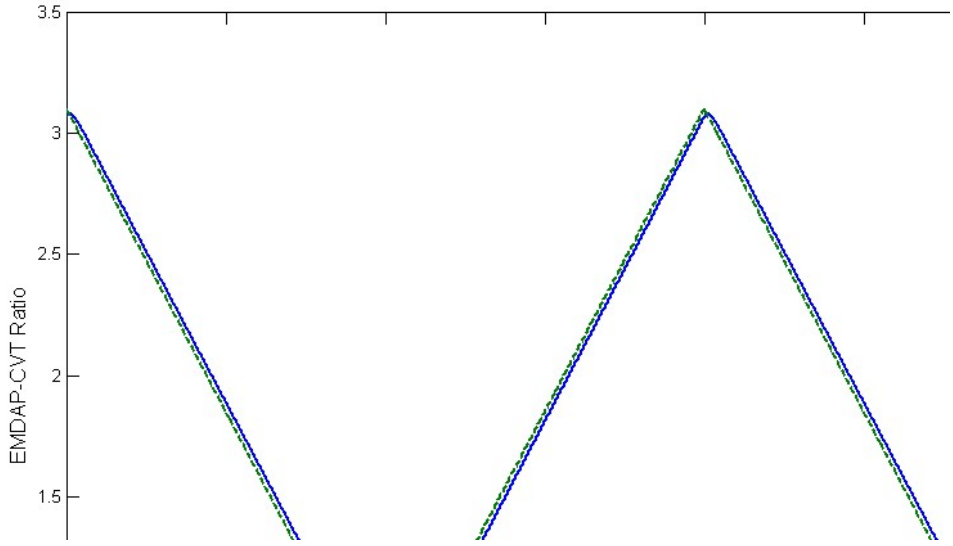

Figure 4.8 The response of PD controller with triangle form input

When the EMDAP-CVT ratio change in a triangular form, the output response of the inner loop system using PD controller with the same gains values is shown to have the ability to track the target ratio as shown in Figure 4.8. Even there is phase shift in the graph, but the error is below 2% or 0.06 EMDAP-CVT ratio and considered as steady state (Dorf and Bishop, 2008). These simulation results also demonstrate that the tracking errors are small, as shown in Figure 4.9. This indicates that the PD controller is suitable for the inner loop controller.

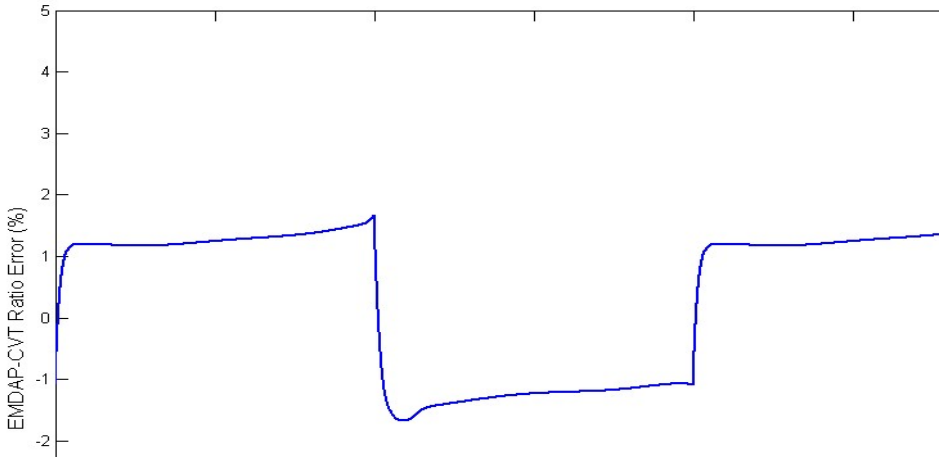

Figure 4.9 Error of the inner loop controller

The drivetrain model with outer loop controller and inner loop controller is studied using two types of controllers and implemented for the outer loop control system. There are the classical PID controller and adaptive ANN. With the same inner loop controller and the same simulation parameters, the performance of each outer loop controller is studied.

4.4 PID Outer Loop Control Scheme

Many researchers used classical controller such as PID for the outer loop controller (Chan *et al*., 1984; Spijker *et al*., 1993; Guzzella and Schimd, 1995). In this section a PID controller is used for the outer loop controller as shown in Figure 4.2. The desired engine speed is calculated based on Figure 3.17 which depends on the throttle opening. At the same time the throttle opening is used as input to the

engine torque table developed in Figure 3.6. The result of the control scheme using PID for the outer loop is important and it will be the bench mark for the proposed control scheme using adaptive artificial neural network (ANN).

4.4.1 Simulation Results

Controlling the engine speed at its desired speed based on the performance driving is the objective of the proposed drivetrain control scheme. To study and evaluate the effectiveness of the outer loop PID controller performance for the drivetrain model, several throttle openings were used. Different road gradients were used as road disturbance that represent a real road condition. Using Simulink program with Heun method, fixed step solver option and single tasking, the simulation results are presented below.

4.4.1.1 Constant Throttle Opening

The outer loop performance using PID controller is shown in Figure 4.10. The throttle opening is adjusted at three different level 15, 40 and 80% respectively. With 0% road gradient the desired engine speed can be achieved in about 100 second. Figure 4.10 shows that the time response for every throttle set is almost similar for throttle opening of 15, 40 and 80%. The desired engine speed can be reached by adjusting the EMDAP-CVT ratio as shown in Figure 4.10(b). At 0% road gradient the steady states are achieved when the EMDAP-CVT ratio is at overdrive position, where the EMDAP-CVT ratio is below 1:1. Figure 4.10(c) shows that the engine speed error is almost equal and reached steady states in 120 seconds. The overall simulation results are acceptable but the output of the outer loop PID controller is chattering as shown in Figure 4.11. This phenomenon occurs at any throttle angle and various road gradients. According to Guzzella and Schimd, (1995), the PID controller is not suitable for non linear equation; this may be the reason why the output of outer loop controller using PID is chattering. Since the output of the

outer loop controller is chattering, implementation in real system will result with poor performance.

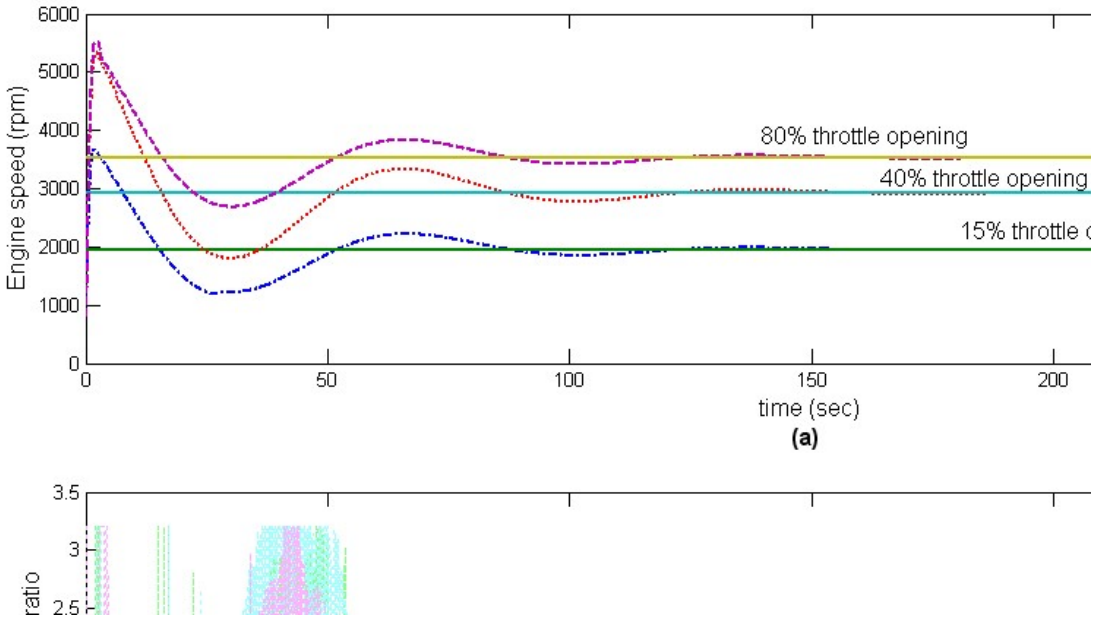

Figure 4.10 PID simulation results for various constant throttle opening at 0% road gradient

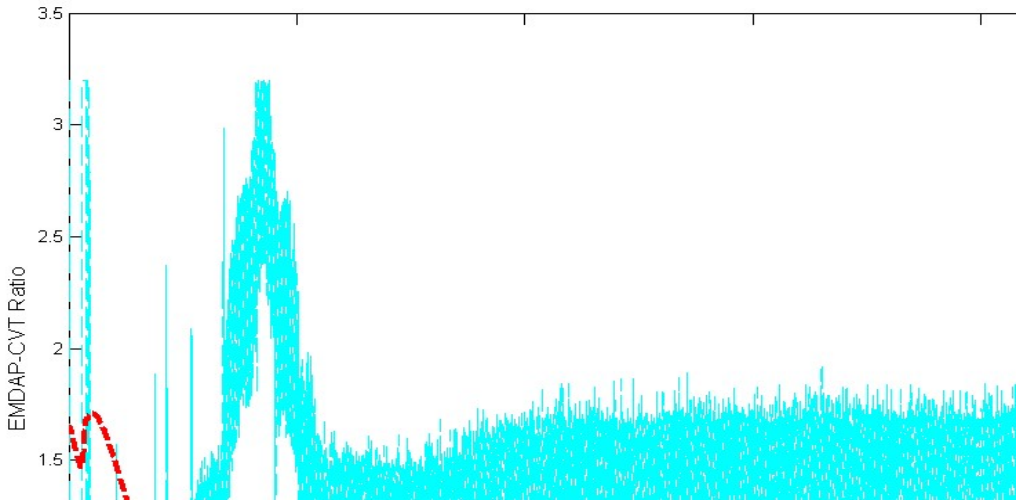

Figure 4.11 The EMDAP-CVT desired ratio and the actual ratio at 40% throttle opening

4.4.1.2 Constant Throttle Opening With Road Gradient Variation

Figure 4.12 shows the simulation result of outer loop controller using PID control system. The throttle is set at 80% and road gradient is assumed to be 3, 5, 7, and 10% inclination. The time response is almost similar for the different road gradients, but the overshoot for every road gradient is slightly different as shown in Figure 4.12(a). The EMDAP-CVT ratio response to keep the engine speed constant at its desired speed is presented in Figure 4.12(b), where the outputs of outer controller are chattering.

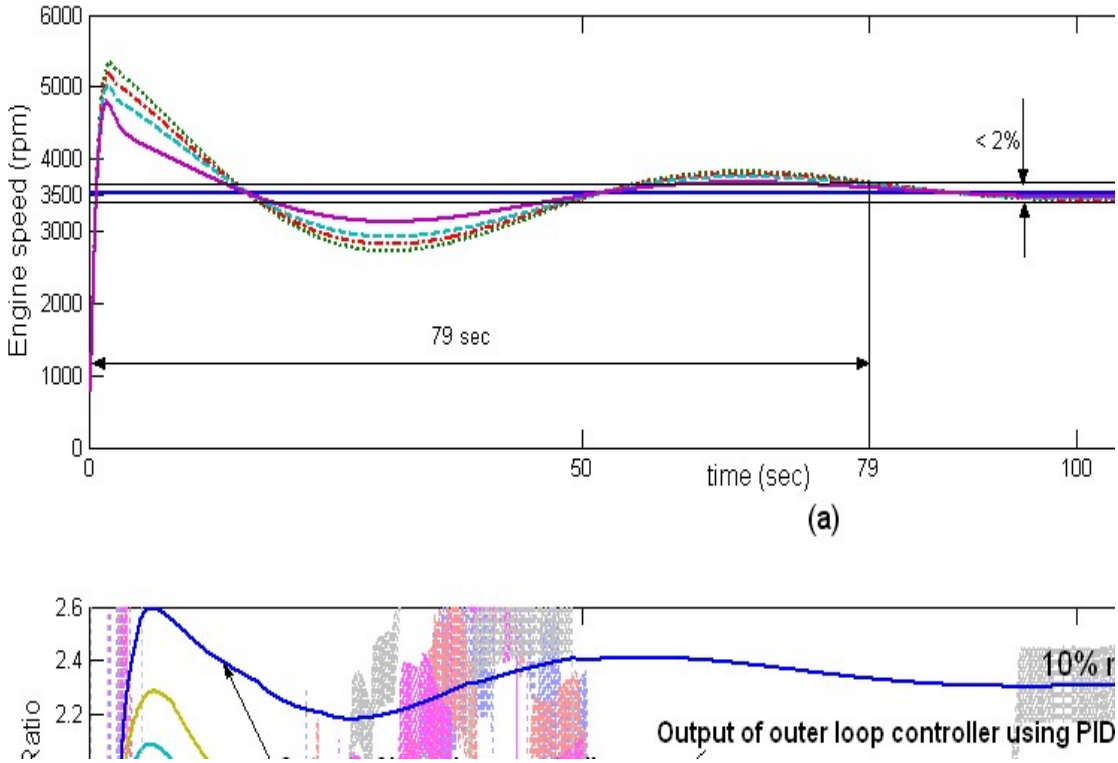

Figure 4.12 Performance of PID controller as outer loop controller at 80% throttle opening with road gradient variation

Figure 4.12(b) shows that high inclination road gradient will increase the EMDAP-CVT ratio. As the road gradient increases, the vehicle load will increase. Hence to overcome the increase load the EMDAP-CVT ratio has to be increased. The vehicle load of 10% load gradient is higher than the vehicle load at 7% road gradient, so that the transmission ratio at 10% road gradient is higher than the ratio at 7% road gradient.

4.4.1.3 Effect of Different Throttle Opening Profile and Road Gradient Variation

To simulate a normal driving condition, the throttle opening is set at three different profiles which are sinusoidal wave, trapezoid wave and mixed profile. Five different road gradients studied are 0, 3, 5, 7 and 10% inclination to test the climbing ability of the vehicle. Figures 4.13(b), 4.14(b) and 4.15(b) show the different responses of the outer loop controller system subjected to different road gradients. Basically these three figures have similar response time, where the desired engine speed can be reached in about 120 second for most of throttle opening. In Figure 4.13(b), the desired engine speed can be reached in 120 second when the road gradient is above 3%. At 0% road gradient, the actual engine speed could hardly to track the desired speed with the same PID gain. This may be due to the vehicle load for 0% road gradient is less and the PID gain has to be readjusted (Guzzela and Schmid, 1995). The outer loop controller output is also chattering as observed in the previous simulation. Similar results were obtained for the other two throttle opening profiles. Figure 4.14(a) shows the trapezoid wave throttle opening, and the desired engine speed can be reached in 120 second as shown in Figure 4.14(b). But for mixed profile throttle opening the desired speed is reached in about 160 second. The mixed profile throttle opening is set between 45 and 90% so that the torque generated by mixed profile throttle opening is also higher. Logically with a higher generated torque the faster will be the response. This indicates that the PID controller is not suitable for nonlinear system. Chattering of the outer loop controller output will make the performance of a real system poor. This simple PID controller in impractical unless a gain scheduled controller as suggested by Guzzela and Schmid (1995) is implemented. Based on their experience with classical control approach the outcome is not very encouraging, unless reinforced with a gain scheduled controller with typically 100 difference gain points. The alternative proposed outer loop controller using ANN will be discussed in section 4.5.

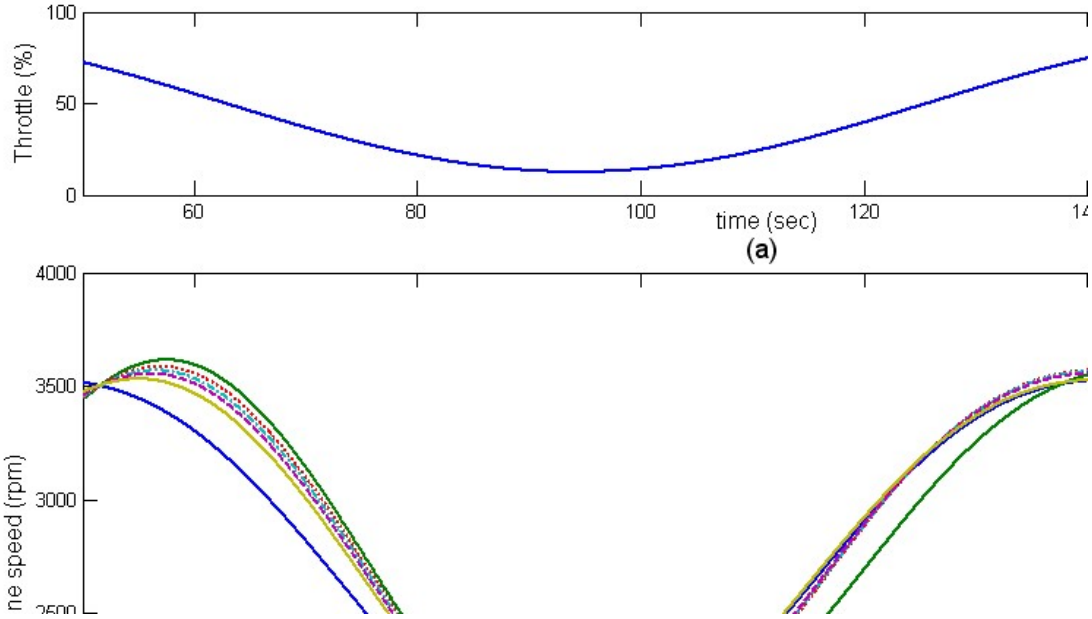

Figure 4.13 Sinusoidal wave throttle opening with road gradient variation using PID controller

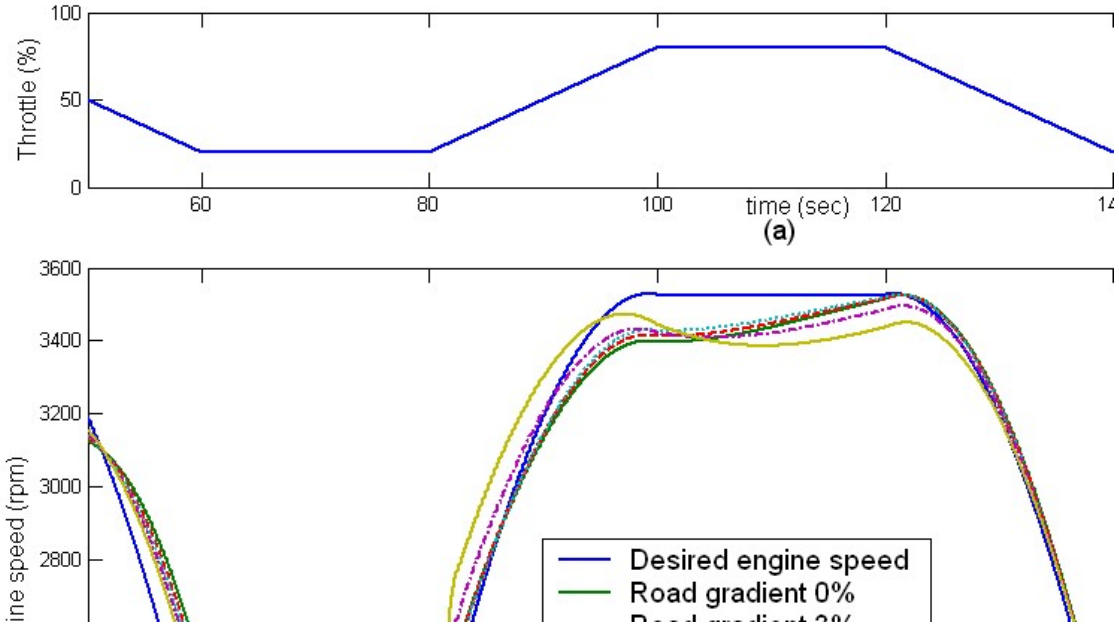

Figure 4.14 Trapezoid wave throttle opening with road gradient variation using PID controller, where the first 100 sec still in transient response.

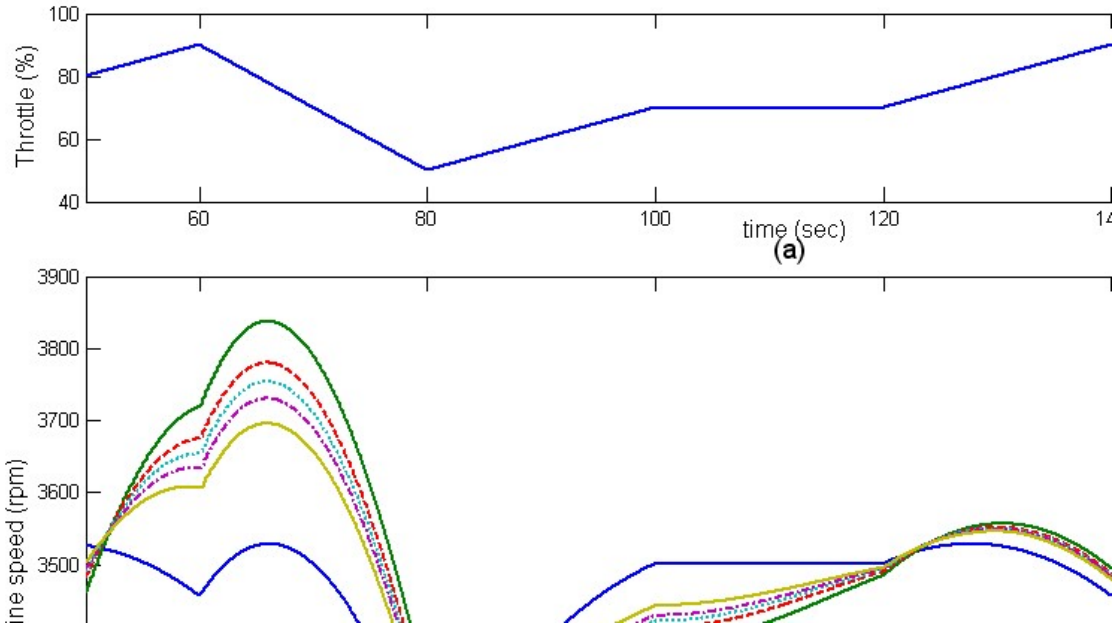

Figure 4.15 Mixed profile throttle opening with road gradient variation using PID controller

4.5 ANN Outer Loop Control Scheme

A linear control system can be designed easily using classical design techniques such as PID, however in drivetrain applications, where the parameters of the system are non-linear in nature, the conventional feedback controller is unable to maintain the desired response. The effect of the parameters variations can be compensated to some extent by a high-gain negative feedback loop, but excessive gain may cause under-damping or instability problem (Pofahl *et al.*, 1998; Bose, 2001; Tsoukalas and Uhrig, 1996).

Plants with parameter variation may require adaptation of the controller parameters in real-time called adaptive control technique (Astrom and Wittenmark, 1995; Narendra and Parthasarathy, 1990; Mills *et al.*, 1996; Gupta and Shinha, 1992 and Lu, 1996). Generally, the adaptive control system can be thought of as having two loops. The first loop is a normal feedback for the process and the other loop is the parameter or mechanism adjustment loop.

Artificial neural network controller is suitable for adaptive control system because it has the ability to process either numerical or linguistic information, and to analyze the input and output simultaneously (Graupe, 1997). Figure 4.16 shows the proposed outer loop controller, where the difference between the output of the plant and the target value is used to adjust the ANN in real time.

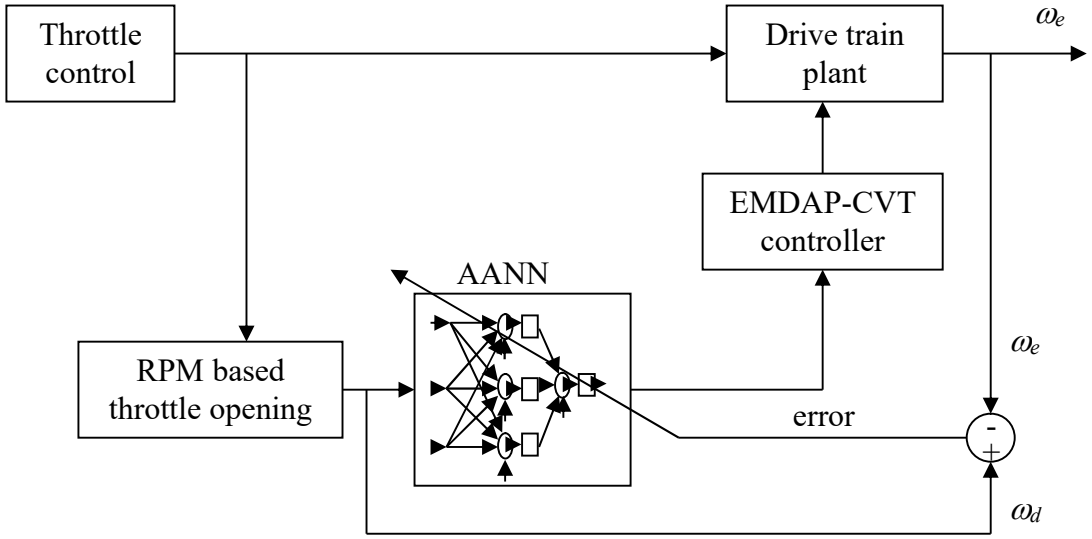

Figure 4.16 The proposed ANN outer loop control system

4.5.1 Simulink Block Diagram for the Outer Loop Control

With the ability to process and analyse input and output information, neural network controller has been shown to be successfully applied to nonlinear and multi-output plants. The drivetrain with EMDAP-CVT is a complex system. This means that the model is a complex non-linear process control, which may require adaptive type controller with adaptive controller parameters update.

The drivetrain model has been discussed in the Chapter 3 and the Simulink block diagram of the outer loop control system is shown in Figure 4.17. The outer loop controller has two inputs, which are the desired engine speed and the actual engine speed which is the output of the drivetrain. There is one output, the desired

EMDAP-CVT ratio. The desired EMDAP-CVT ratio is then used by the inner loop control as its input.

An S-function block was used in the Simulink block diagram for ANN controller. The S-function diagram was built based on the ANN architecture, which will be discussed in section 4.5.2. The simulation will be focused on the actual engine speed and the error of both the outer loop and inner loop controller outputs (Mościński and Ogonowski, 1995).

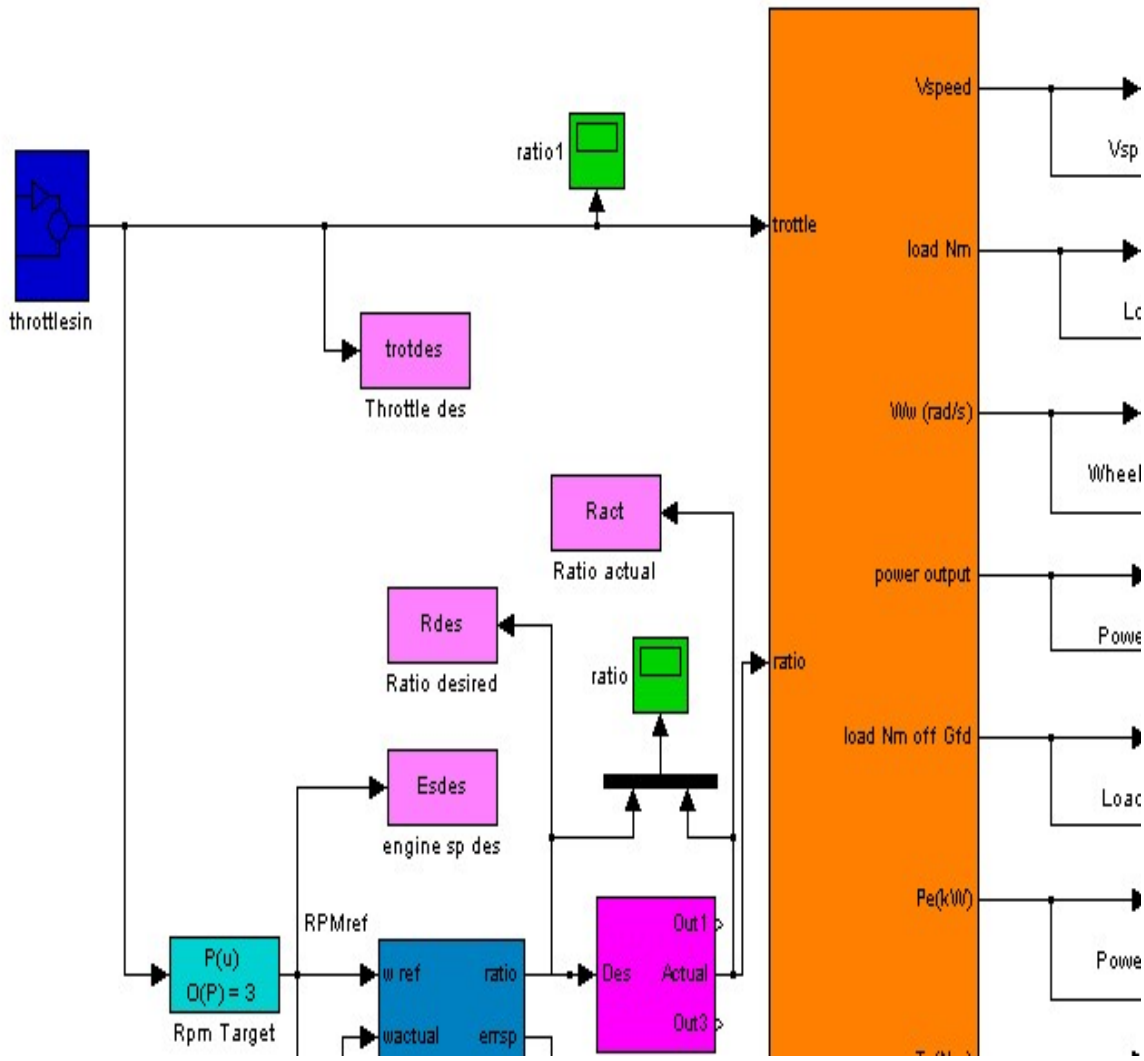

Figure 4.17 Simulink block diagram of ANN outer loop control system

The working principle of the simulation model can be explained as follow. The throttle opening was set to a certain value and referring to Figure 3.18 the desired engine speed can be determined. This engine speed is the reference speed of

the adaptive neural network controller to be tracked by adjusting the ratio of the EMDAP-CVT. When the throttle opening is kept constant, based on the control rule discussed in section 4.2, the output of the ANN is the EMDAP-CVT ratio that will minimise the error between the target engine speed and the actual engine speed. The output of the outer loop controller is the desired ratio needed by the inner loop controller.

4.5.2 Neural Network Architecture

An artificial neural network consists of a large number of very simple and highly interconnected processors, also called neurons. The neurons are connected by weighted links passing signals from one neuron to another. Each neuron may receive a number of input signals through its connections: however, it does not produce more than a single output signal. The output signal is transmitted through the neuron's outgoing connection, which in turn, splits into a number of branches that transmit the same signal.

Neural network may be classified as a single layer or multilayer network. In determining the layer, the input units are not counted as a layer, because they perform no computation. The number of layers is defined by the number of layers of weighted interconnected links between the slabs of neurons.

A neuron is just a function of the weighted sum of its inputs. Figure 4.18 shows the proposed network architecture with one hidden layer for the outer loop drivetrain controller. The theoretical result presented by Fausett (1994) shows that one hidden layer is sufficient for the network to approximate any continuous mapping from the input patterns to the output patterns to an arbitrary degree of accuracy. The output can be expressed as follow:

$$Y = f\left(\sum_{i=0}^{n} w_i O_i + b\right) \tag{4.3}$$

where,

f : the activation function

w_i : the weight connection

b : the bias.

Appropriate weights for the connection need to be defined. Learning algorithm such as back-propagation may be used to train the weight (Rumelhart *et al*., 1986; Liu and Kadirkamanathan, 1995). The sigmoid activation function is expressed as:

$$f(x) = sigmoid(x) = \frac{1}{1 + e^{(-\frac{x}{T})}}, \quad T > 0 \tag{4.4}$$

For the sigmoid function, note that if $T \rightarrow \infty$, then $f(x)$ tends to a linear function while if $T \rightarrow 0$, then $f(x)$ tends to a sign function. This function is, in fact, the logistic function, one of the several sigmoidal function which monotonically increase from a lower limit (0 or –1) to an upper limit (+1) (Omatu *et al*., 1996).

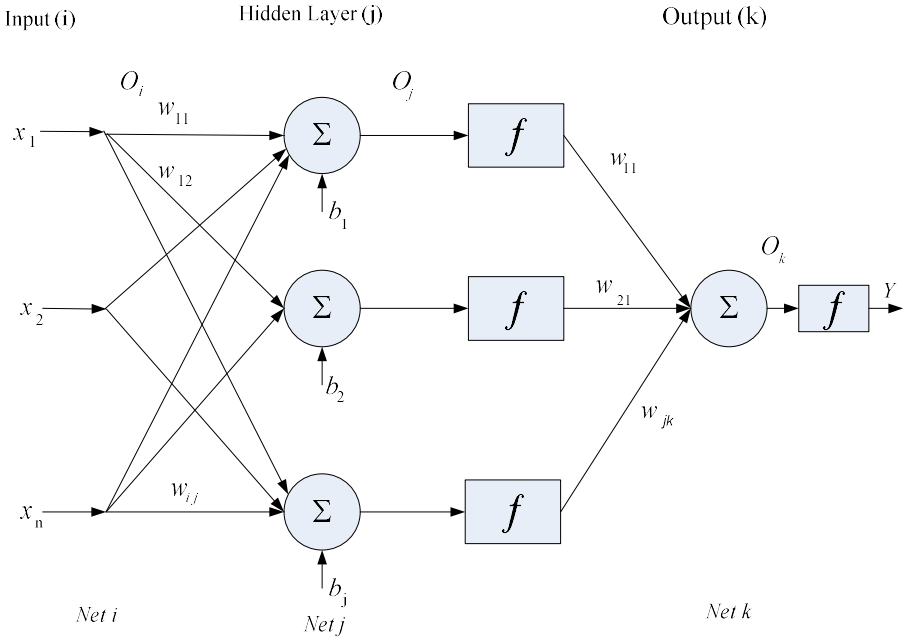

Figure 4.18 A multilayered structure of neuron

4.5.2.1 Algorithm: Backpropagation Method

The backpropagation is based on the steepest descent (gradient) algorithm to find the minimum of the error. The backpropagation algorithm can be summarised with the following steps (Omatu *et.al.*, 1996):

Step 1. The initial value of weight, w_{kj}, bias, b_j, and learning rate, α, are set.

Step 2. The inputs ω_d and ω_e are applied to the neural network, the corresponding desired output, υ, is specified and O_j, O_k, and δ_k are calculated with

$$\delta_k = \left(1 - O_k^{\,2}\right)\left(\upsilon - O_k\right) \tag{4.5}$$

Step 3. The connection weights at layer k is changed by

$$\Delta w_{kj}(t+1) = \delta_k O_j + \alpha\, \Delta w_{kj}(t) \tag{4.6}$$

Step 4. The output δ_j is calculated using

$$\delta_j = \left(1 - O_j^{\,2}\right) \sum_k \delta_k w_{kj} \tag{4.7}$$

Step 5. The connection weights and bias at hidden layer ji are changed using

$$\Delta w_{ji}(t+1) = \delta_j O_i + \alpha \Delta w_{ji}(t) \tag{4.8}$$

$$\Delta b_j(t+1) = b_j(t) - \alpha\, \Delta b_i(t) \tag{4.9}$$

Step 6 $t \rightarrow t + 1$ and step 2 is repeated until Δw and $\Delta b \rightarrow 0$

4.5.3 Determination of ANN Structure for Outer Loop Controller

The proposed control system as shown in Figure 4.16 and ANN structure shown in Figure 4.18 was studied using 5 different ANN structure for engine speed control. Figure 4.19 shows the architecture of a typical one hidden layer network with different number of nodes in the hidden layer.

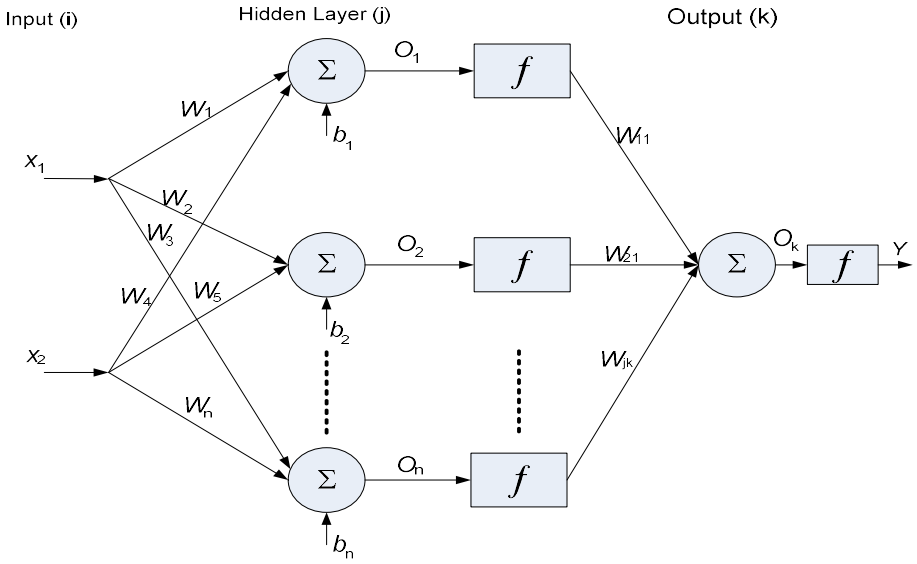

Figure 4.19 An ANN with two input and single hidden structure

The proposed structure with different nodes is implemented in the drivetrain model and run with the same conditions. The throttle was set at constant value of 40% and road gradient is set to 5, 3% inclinations and 1% declinations, respectively. All the five different nodes network are found to be able to keep the engine speed at its desired value but with different root mean square error (RMS) of the output speeds. The RMS error values are 796, 779, 666, 687 and 736 for network in 1, 2, 3, 4, and 5 nodes respectively. Figure 4.20 shows the relation between the number of nodes and the RMS error.

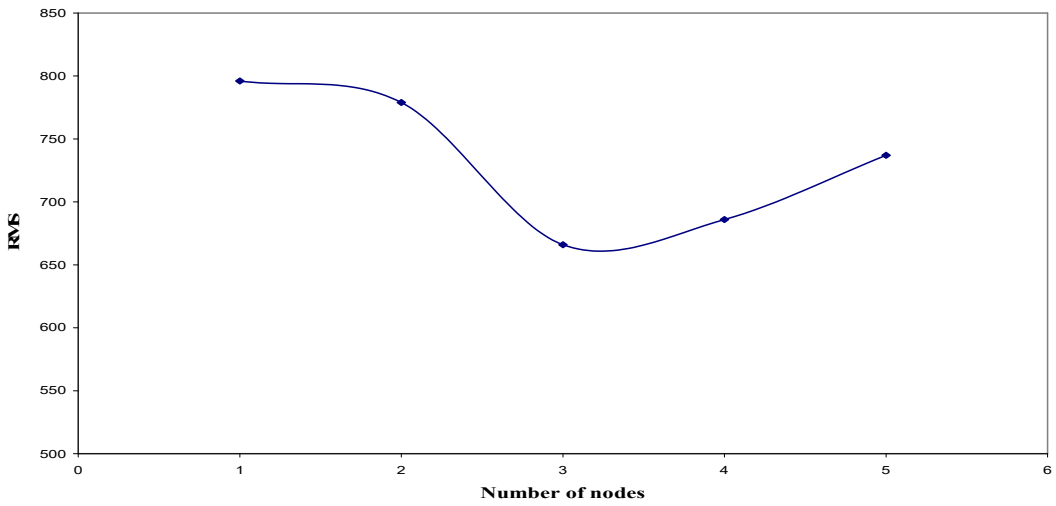

Figure 4.20 Root mean square (RMS) error for ANN controller with different number of nodes

Figures 4.21, 4.22 and 4.23 show the result of adaptive ANN response with different number of hidden nodes. Only three different hidden node networks which have small RMS error values are presented to study the performance of the drivetrain system. The results show that the time responses are almost similar. When the road inclination changed to 5% the engine speed slows down and quickly returns to the desired speed. The EMDAP-CVT ratio is adjusted to keep the engine speed at its desired speed as shown in Figures 4.21(d), 4.22(d) and 4.23(d). When the road gradient changes from 5 to 3% the vehicle load will decrease. The actual engine speed is faster for a few seconds before it returns back to its desired speed. The time responses due to the road gradient change are about the same for the three different hidden node networks. The engine error responses are almost similar as shown in Figures 4.21(c), 4.22(c) and 4.23(c), but the RMS errors are different. Figure 4.20 shows the 3 hidden nodes adaptive ANN structure has the minimum RMS error compared to the other four structures. Hence the adaptive ANN with one hidden layer and 3 nodes is selected to be implemented for the outer loop controller.

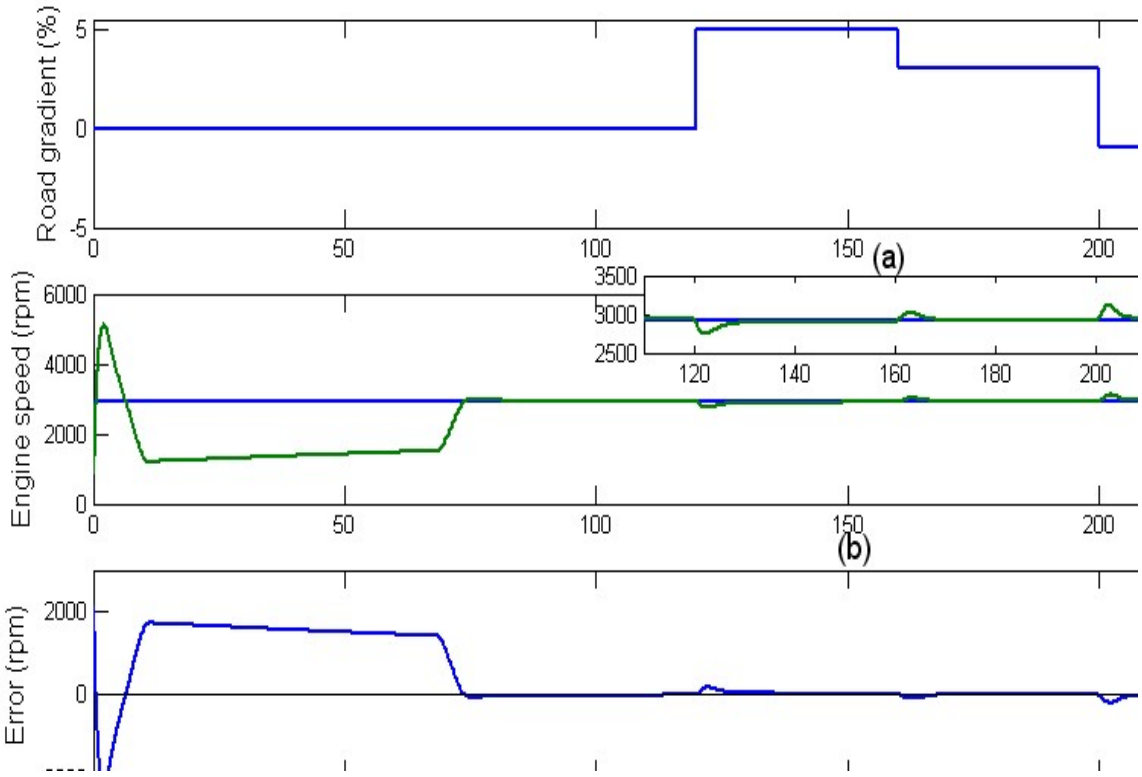

Figure 4.21 Response time of adaptive ANN structure with 3 hidden nodes

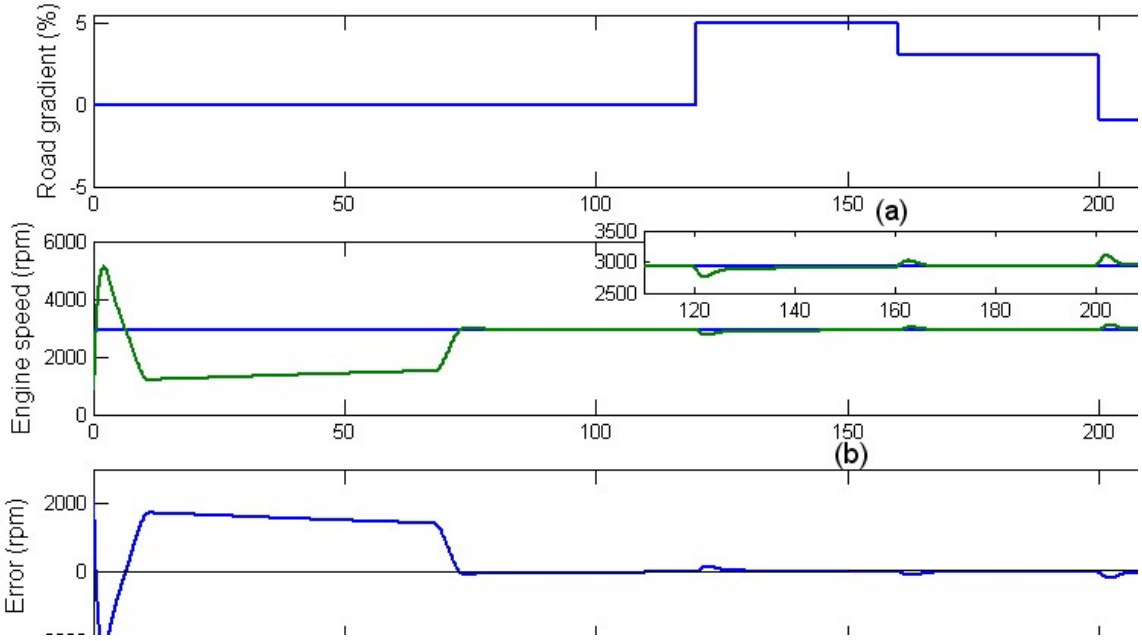

Figure 4.22 Response time of adaptive ANN structure with 4 hidden nodes

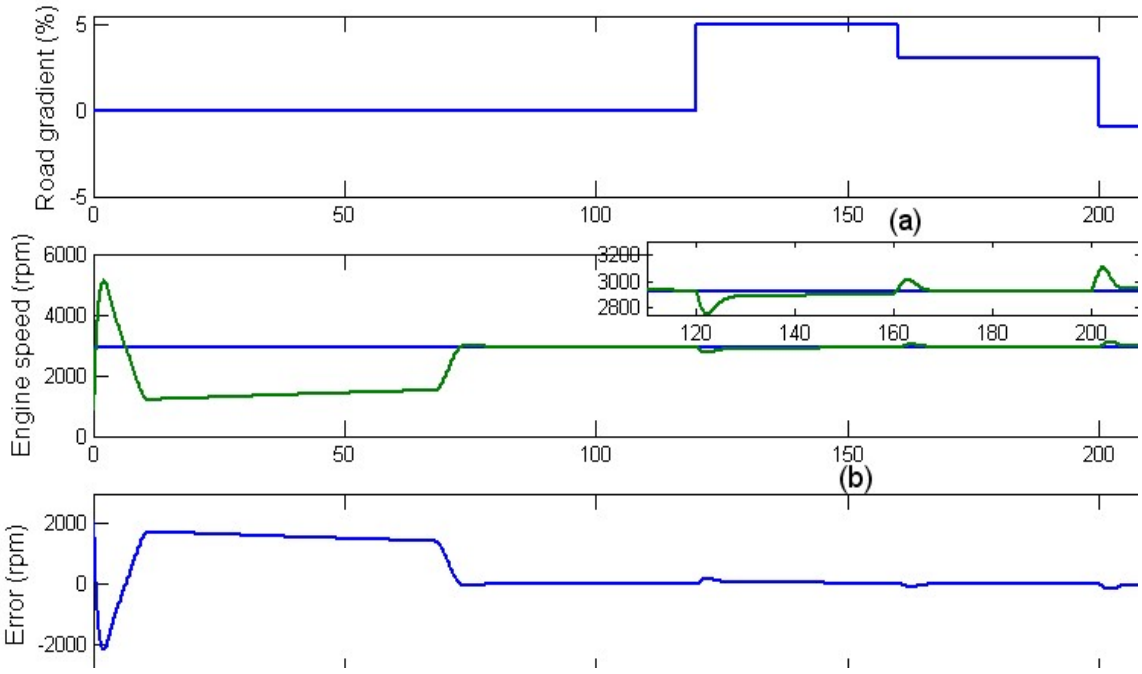

Figure 4.23 Response time of adaptive ANN structure with 5 hidden nodes

Figure 4.24 shows the variation of the weight and threshold for the 3 hidden node network adaptive ANN structure during the training process, where the convergences are clearly shown. This indicates that adaptive ANN has updated its parameters that resulted with an optimal controller for the drivetrain system.

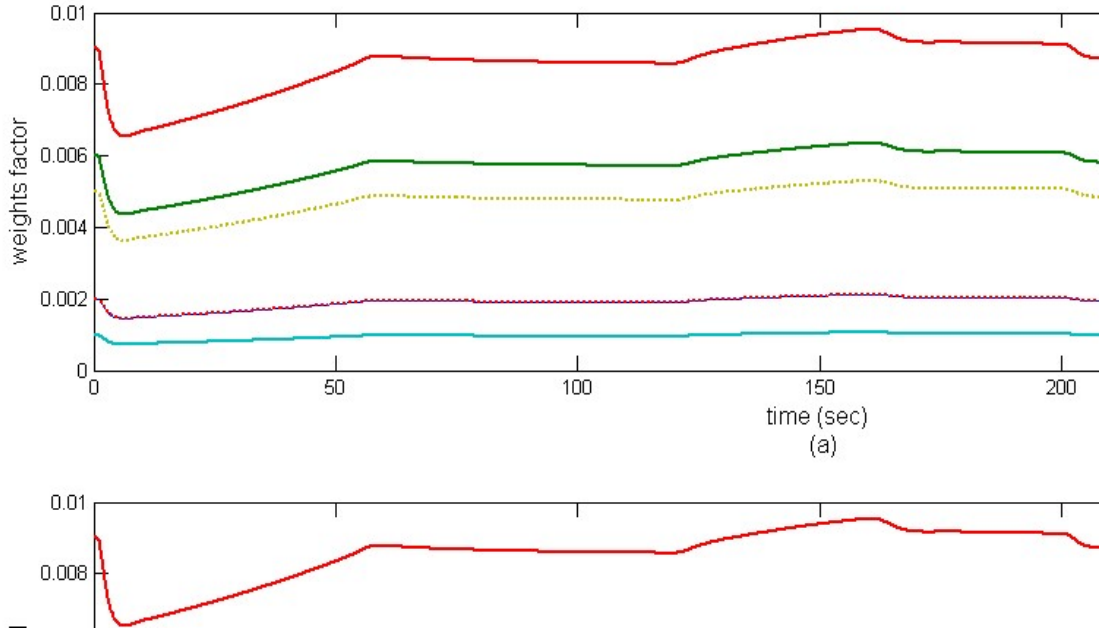

Figure 4.24 Adapted 6 weights factor and 3 threshold for 3 nodes adaptive ANN

4.6 Simulation Results

To study the ability of the outer loop controller using adaptive ANN with 3 hidden nodes, various conditions are considered. The first condition is to use constant throttle, which represents a vehicle running on a highway. The second condition is to vary the throttle opening with three different levels of throttle opening that may representing on urban or a country road with different road inclinations and windings.

4.6.1 Constant Throttle Opening

The performance of the outer loop controller using adaptive ANN with three node networks was studied by considering different road conditions and different constant throttle opening. The first simulation test was done by using 3 different constant throttles opening with road gradient of 0%. The second simulation test was done by using 4 different road gradients but the throttle opening was kept constant.

4.6.1.1 Constant Throttle Opening With Road Gradient 0%

Figure 4.25 shows the simulation results for three different constant throttle openings set at 15, 40 and 80% respectively. By assuming the vehicle runs at a 0% road gradient, the response of the outer loop controller reached the desired engine speed with various response times depending on the degree of throttle opening. Figure 4.25(a) shows that for a higher value of throttle opening, the response times is faster but with overshoot. This is due to a large torque delivered by the engine for a larger throttle opening.

Figure 4.25(b) shows the performance of the inner loop controller, where the output of the outer loop controller is the desired ratio can be tracked by the output of

the inner loop controller. This cannot be achieved by the PID controller as presented earlier.

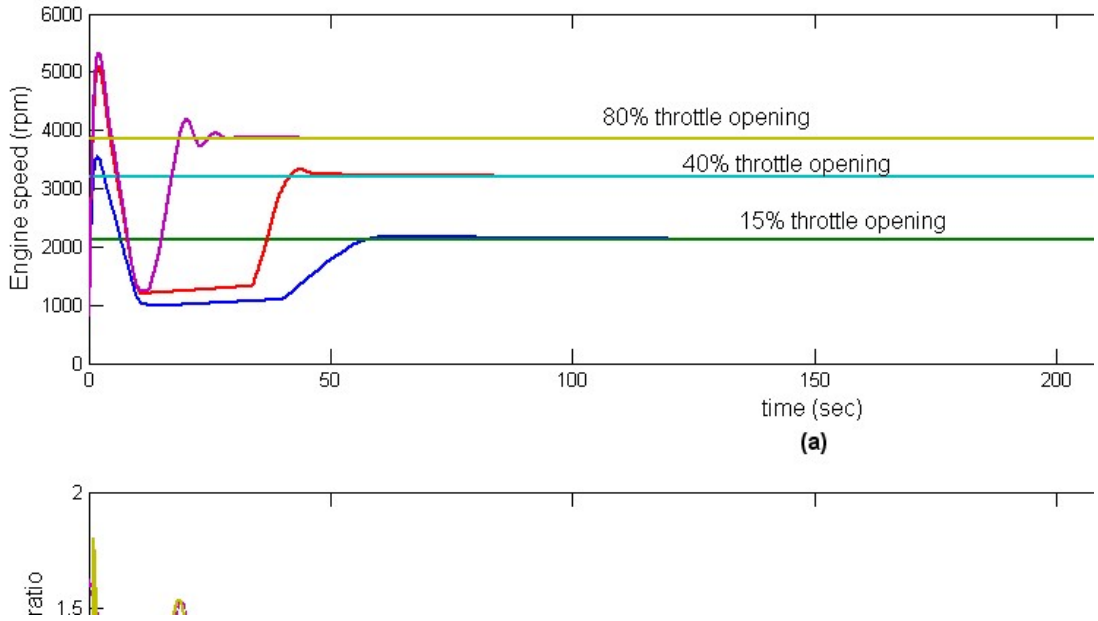

Figure 4.25 Simulation results with various constant throttle opening at road gradient 0%

4.6.1.2 Constant Throttle Opening With Variation of Road Gradient

Figure 4.26 shows the simulation results of the effect of constant throttle opening with various road gradients. The road gradients are set to 3, 5, 7 and 10% and the throttle opening is set at 80% where the target engine speed is 3526 rpm. Dorf and Bishop (2008) states that the settling time is defined as the time required for the system to settle within a 2% percent error of output steady-state amplitude. The graph shows that the outer loop controller is able to reach the target engine speed of about 10 second except for the 10% road gradient. This may due to the performance of the small engine used which has the maximum torque of 43 Nm to overcome the external load caused by the 10% road gradient. Comparing with PID controller for the outer loop control as shown in Figure 4.12, the actual engine speed oscillate for all road gradient. Thus the adaptive ANN is more suitable for this type of non-linear system.

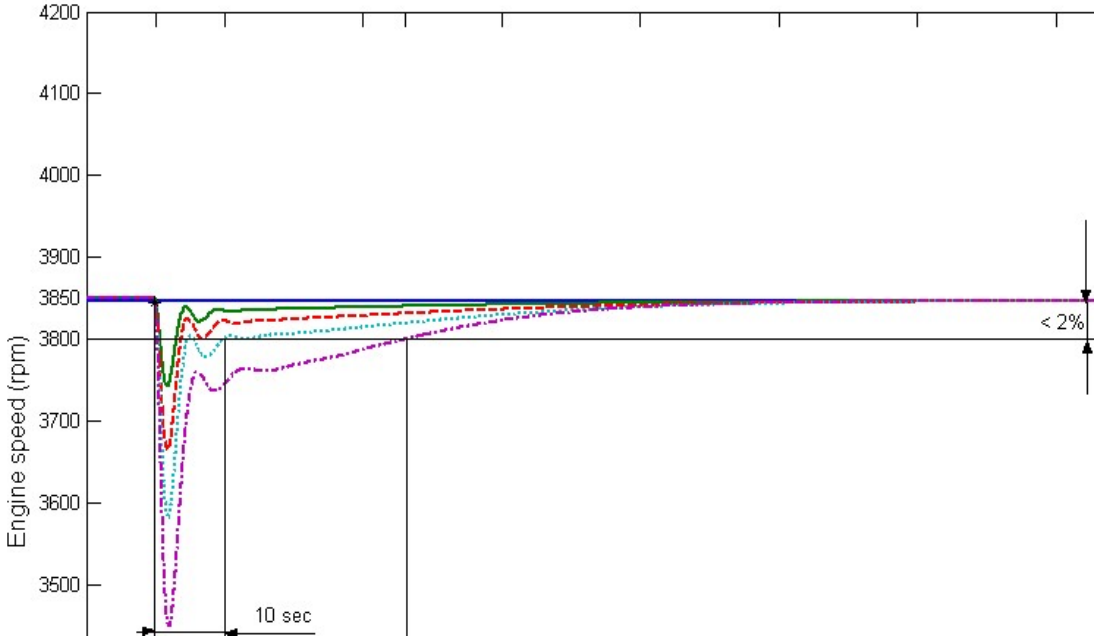

Figure 4.26 Performance of adaptive ANN controller for constant throttle and various road gradients

4.6.2 Variable Throttle Opening

The purpose of this study is to show that the proposed controller works well and the actual engine speed tracks the desired speed when subjected to different road gradient although arbitrary throttle opening is used. This will show the effectiveness of the proposed controller.

During manual driving, drivers do not keep the throttle at a constant opening at all time. The throttle is changed according to road conditions. Therefore, the performance of the outer loop controller subjected to various throttle opening and road conditions is studied. With three different types of throttle opening profile to represent the behaviour of the driver are sinusoidal wave form, pyramidal form and mixed profile throttle opening. Five different road gradients studied are 0, 3, 5, 7 and 10% inclinations.

4.6.2.1 Effect of Throttle's Openings with Constant Road Gradient

Figures 4.27(b), 4.28(b) and 4.29(b) show the different responses of outer loop controller due to variable throttle openings as shown in Figures 4.27(a), 4.28(a) and 4.29(a) and for different road gradients. Basically these three figures have similar responses indicating that the outer loop controller works well to keep the engine speed at its desired speed based on the target line by adjusting the EMDAP-CVT ratio. Especially when the road gradient is under 5%, the outer loop controller is able to maintain the actual engine speed equal to the desired speed.

The dotted lines in Figures 4.27(b), 4.28(b) and 4.29(b) are the responses of the outer loop controller when the vehicle climbs an inclined road with the gradient of 10%. The graph shows that the engine speed oscillates before reaching steady state. Riding the vehicle with small engine to clime the incline road of 10% is hard to reach steady state due to under power of the vehicle engine. The first two throttle opening profiles have minimum value of 20%, indicating that the torque generated is not enough to overcome the vehicle load. Thus the outer loop controller is not able to reach the target engine speed. This phenomenon can be seen clearly in Figures 4.27(b) and 4.28(b) when the engine speed is at the minimum point. Whereas in Figure 4.29(b) the error between the actual engine speed and the desired speed is lesser at the minimum point because the throttle opening is 40% will generate torque that is sufficient to overcome the vehicle load during climbing the incline road of 10%. Therefore it can be concluded that for steeper road gradient the throttle needs larger of throttle opening.

With the oscillation of engine speed less than 2%, it is considered as steady state (Dorf and Bishop, 2008). Comparing with PID outer loop controller, the fluctuation in engine speed is larger, but when the output of PID outer loop controller is chattering as seen in Figure 4.12, which will not be practical in a real system.

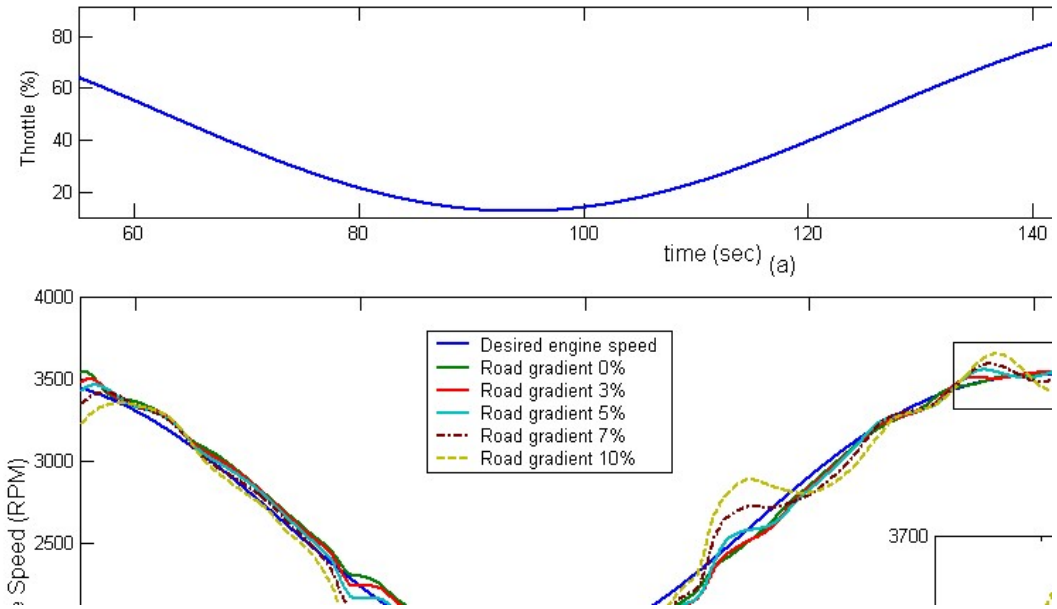

Figure 4.27 Sinusoidal wave throttle opening with different level road gradients

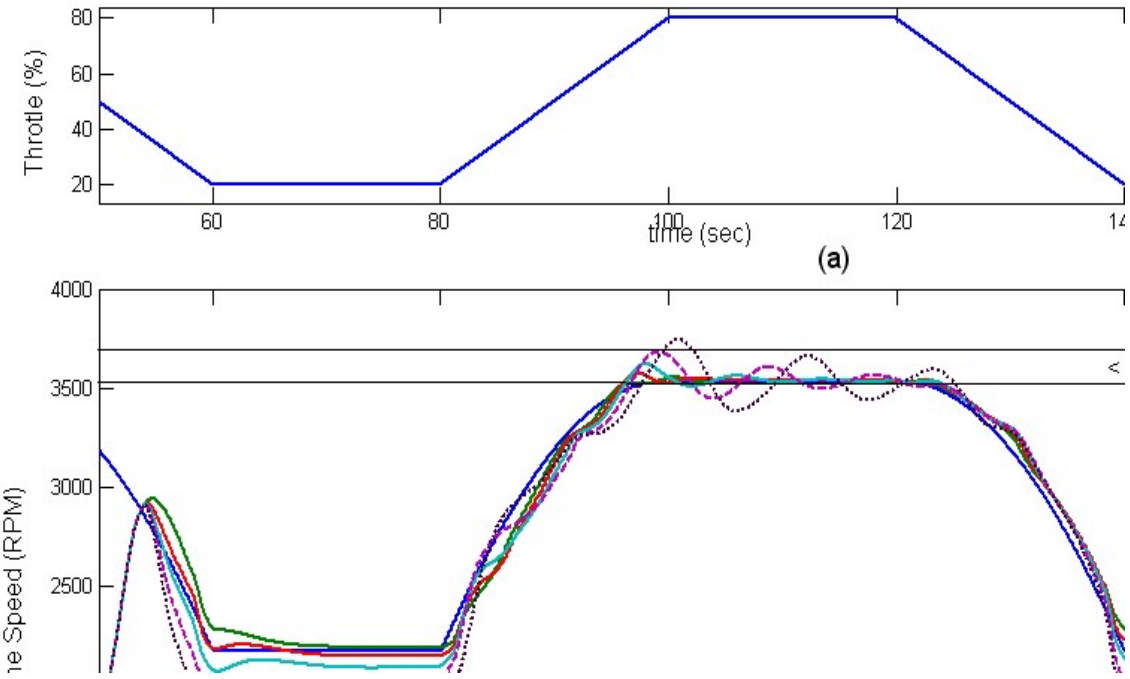

Figure 4.28 Trapezoid wave throttle opening with different level road gradients

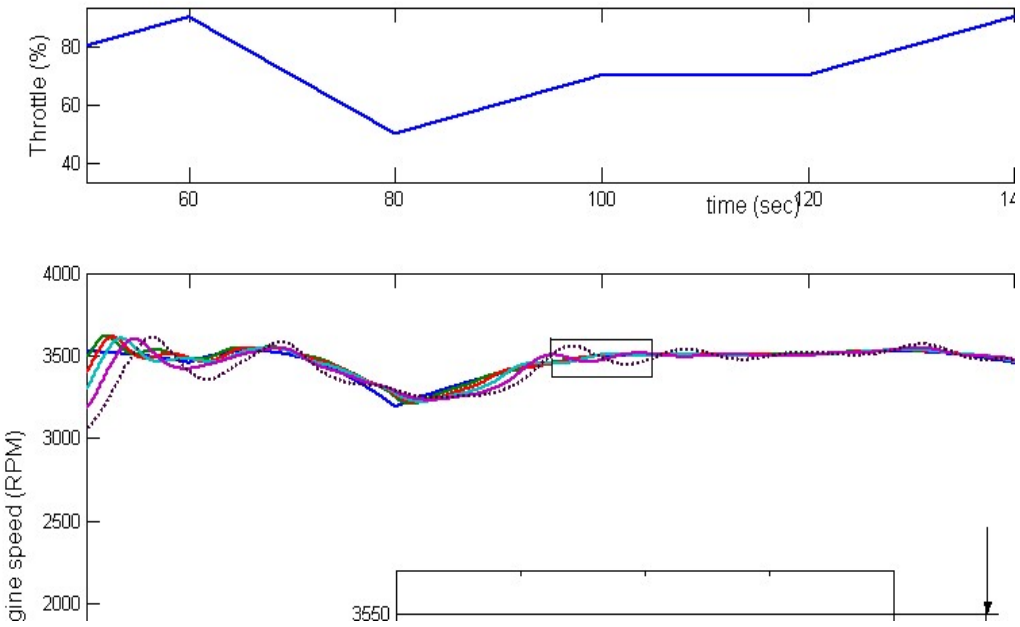

Figure 4.29 Mixed profile throttle opening with different level of road gradients

4.6.2.2 Effects of Throttle Opening With External Disturbance Due to Different Road Gradient

In this section the effects of road gradient are studied for three different throttle opening profiles as shown in Figures 4.30(a), 4.31(a) and 4.32(a). Figures 4.30(b), 4.31(b) and 4.32(b) show the road gradient profile, where the inclination of 9% occur after 120 second forcing the vehicle to climb the road with various throttle opening. After 160 second the road gradient is reduced to 5%, and 40 second later the road declination is 2%.

Figures 4.30(c), 4.31(c), and 3.32(c) show the desired and the actual engine speeds at different throttle openings. Generally, it can be seen that the actual engine speed can track the desired speed. At certain point the actual engine speed are out of the target speed especially when there is a sudden change in the road gradient.

Figures 4.30(d), 4.31(d), and 4.32(d) show the outer loop controller output as the desired ratio which is then used by the inner loop controller. The dash line of these graphs (red dotted line) is the desired ratio when the vehicle runs at 0% road gradient. The overlap green line is the desired ratio needed to satisfy the road gradients profile.

Figure 4.30 shows the performance of the outer loop controller when the throttle opening is a sinusoidal wave. The actual engine speed can track the desired speed by adjusting the EMDAP-CVT ratio. When the road inclination is 9% the engine load also increases causing the actual engine speed to slow down. At the same time the throttle is opened wider so that the engine speed error is reduced as shown in Figure 4.32(a and c). The outer loop controller adjusts the desired ratio from 0.8:1 to 1.8:1 to reach the target speed. When the road gradient changes to 5% inclination, the actual engine speed suddenly increases so that the outer loop controller has to increase the desired ratio to 1.4:1 to reach the desired speed. Since the target engine speed is always changing, the outer loop controller has to adjust the desired ratio continuously.

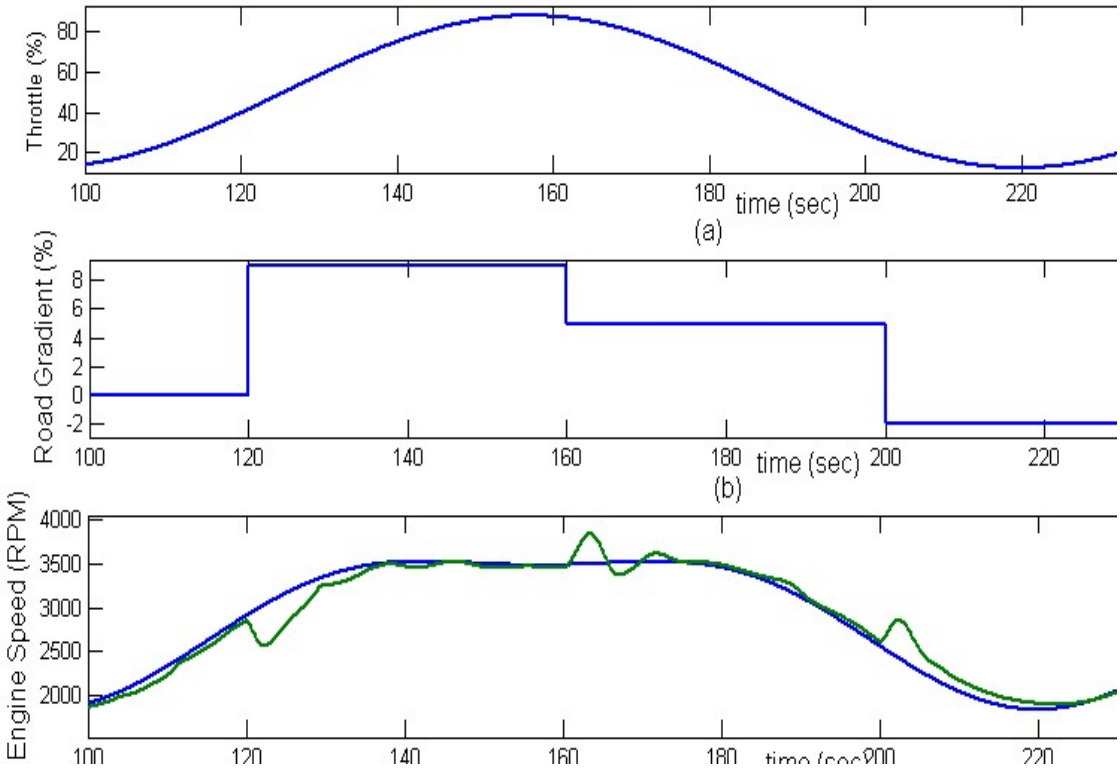

Figure 4.30 Sinusoidal wave throttle opening with different road gradients

Figure 4.31(a) shows the throttle opening set as a pyramidal wave profile and the performance of the outer loop controller. When the road inclination is 9%, the throttle angle is about to decrease and the target engine speed is also decreasing. The inclined road causes the engine speed to reduce, hence the actual engine speed reach the target engine speed faster than in Figure 4.30. At minimum throttle opening the road is still inclined that causes the actual engine speed to slow down. This is due to the torque delivered by the engine is not enough to overcome the road load. Contrary to this condition, at the second minimum throttle opening the road gradient declined by 2%, which reduce the road load, hence the actual engine speed is closer to the target speed.

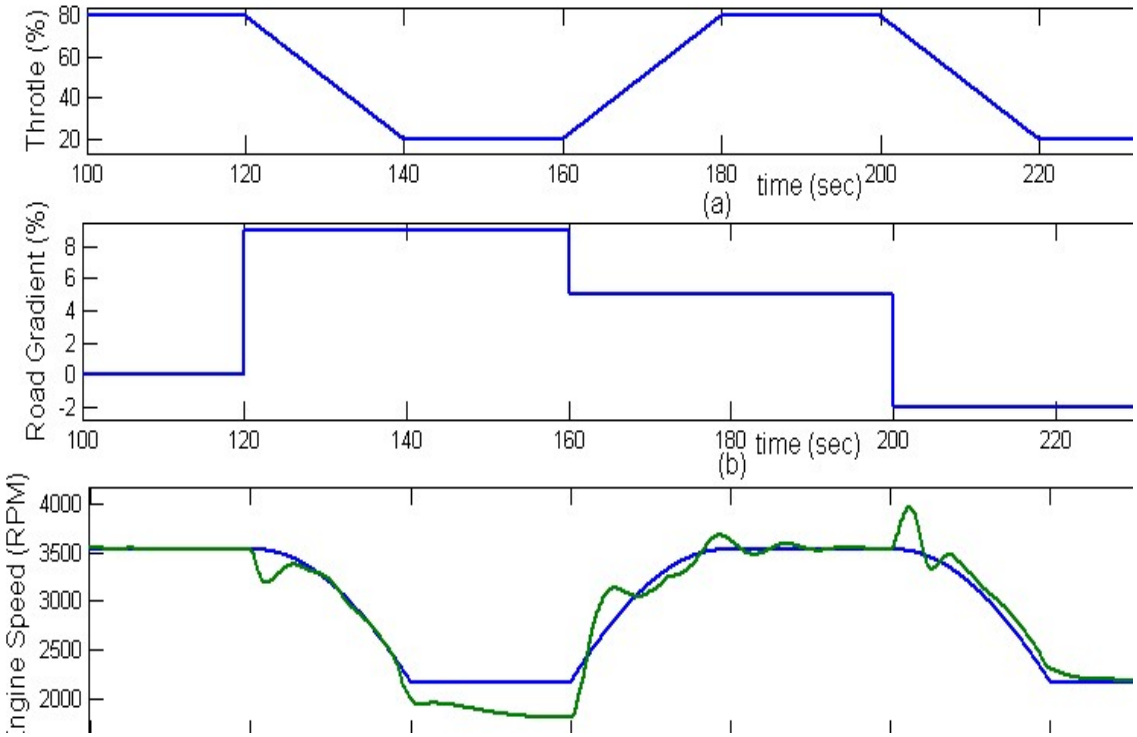

Figure 4.31 Pyramidal wave throttle opening with different road gradients

Figure 4.32(c) shows the outer loop controller adjusts the EMDAP-CVT ratio by reducing the gear ratio until the actual engine speed reaches the desired speed even though the road has inclination of 9%. When the inclination of the road equals to 5%, the vehicle load also decreases so that the engine speed increases for awhile before the outer loop controller increase the EMDAP-CVT ratio to keep the engine

speed at its desired value. Similarly when the road gradient is declined by 2%, the actual engine speed is higher than the desired speed. When the road gradient decreases the vehicle load reduces. This phenomenon is indicated by the increase in engine speed. Increasing the EMDAP-CVT ratio by the outer loop controller can maintain the engine speed at its desired ratio.

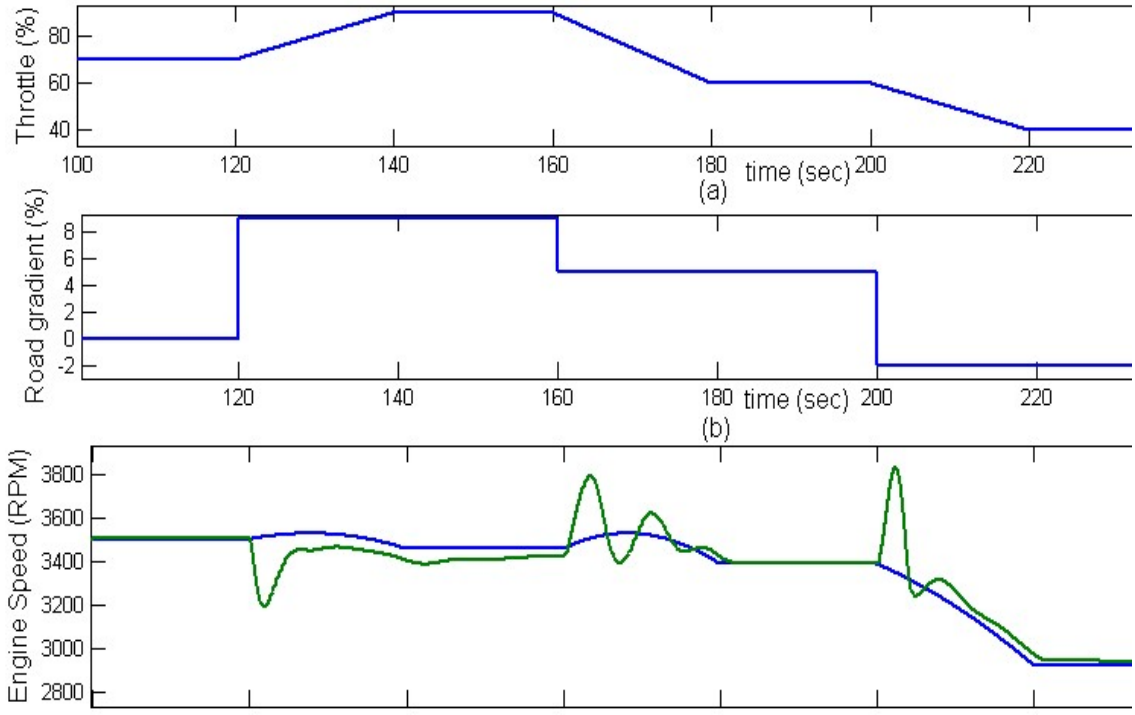

Figure 4.32 Mixed profile throttle opening with different road gradients

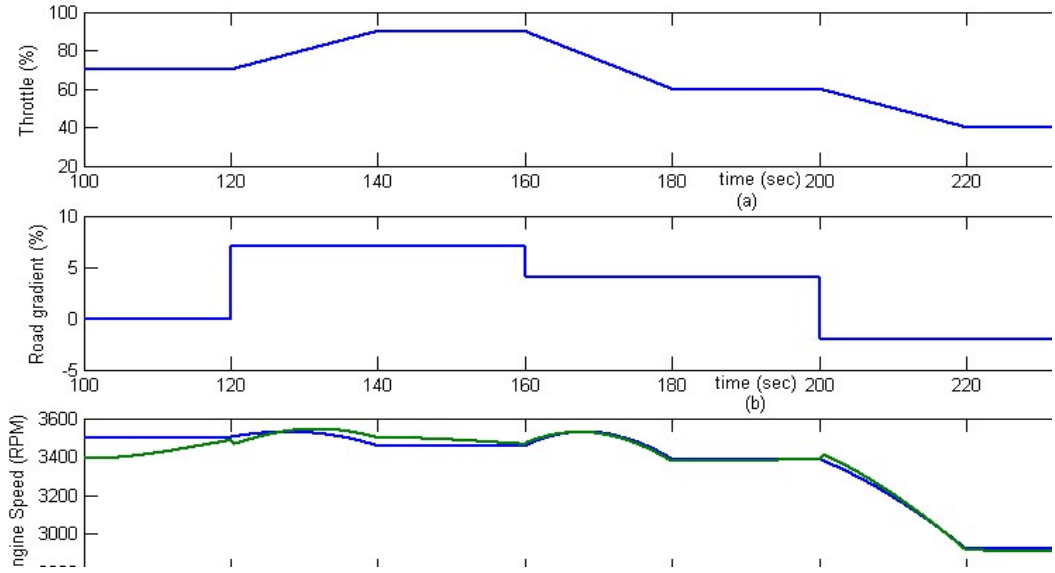

Figure 4. 33 Mixed profile throttle opening with different road gradients using PID controller

4.7 Summary

The simulation study of the control scheme for the drivetrain model has been presented, where the controller consists of two loops. These are outer loop controller and inner loop controller. The PID and adaptive ANN have been used to control the outer loop controller. The simulation result shows that both controllers are able to keep the engine speed in its desired, but the output outer loop controller using PID shows chattering. Figure 4.33 show the simulation results with mixed throttle opening and various road disturbances. The output of the outer loop controller is chattering as seen in Figure 4.33(d) and implementation in real system will result with poor performance. Whereas the output of the outer loop controller using adaptive ANN is more acceptable to be implemented in the real system as seen in Figure 4.32(d). Therefore, the proposed outer loop controller is the adaptive ANN and the inner loop controller is the PD type controller. The simulation results show that both controllers work well and able to overcome external disturbance.

The major contribution of this chapter is the use of adaptive ANN applied to the drivetrain model equipped with EMDAP-CVT. Using simple ANN architecture consisting of three hidden nodes single layer network, this adaptive ANN has the ability to produce the desired EMDAP-CVT ratio so that the engine rpm can be maintained according to the desired engine rpm. This control strategy will then be applied to an experimental rig discussed in the next chapter.